Interactions of the GM2 Activator Protein with Phosphatidylcholine Bilayers: A Site-Directed Spin-Labeling Power Saturation Study

Jordan D. Mathias, Yong Ran, Jeffery D. Carter, and Gail E. Fanucci*
Department of Chemistry, University of Florida, Gainesville, Florida

ABSTRACT The GM2 activator protein (GM2AP) is an accessory protein that is an essential component in the catabolism of the ganglioside GM2. A function of GM2AP is to bind and extract GM2 from intralysosomal vesicles, forming a soluble protein-lipid complex, which interacts with the hydrolase Hexosaminidase A, the enzyme that cleaves the terminal sugar group of GM2. Here, we used site-directed spin labeling with power saturation electron paramagnetic resonance to determine the surface-bound orientation of GM2AP upon phosphatidylcholine vesicles. Because GM2AP extracts lipid ligands from the vesicle and is undergoing exchange on and off the vesicle surface, we utilized a nickel-chelating lipid to localize the paramagnetic metal collider to the lipid bilayer-aqueous interface. Spin-labeled sites that collide with the lipid-bound metal relaxing agent provide a means for mapping sites of the protein that interact with the lipid bilayer interface. Results show that GM2AP binds to lipid bilayers such that the residues lining the lipid-binding cavity lie on the vesicle surface. This orientation creates a favorable microenvironment that can allow for the lipid tails to flip out of the bilayer directly into the hydrophobic pocket of GM2AP.

INTRODUCTION

Gangliosides are sialic-acid-containing glycosphingolipids that are found in elevated concentrations in the outer membrane of neuronal cells, which function as cell markers, binding sites for viruses and bacterial toxins, and coreceptors for various hormones, as examples (1). Catabolism of gangliosides is a vital cellular process that occurs in the lysosomal compartments of cells where the sequential cleavage of terminal sugar residues proceeds via enzymatic degradation by >10 different exohydrolases resulting in the production of ceramide. Upon removal of the fatty acid chain by acid ceramidase, ceramide is further degraded to sphingosine (2). The degradation of gangliosides that contain four or fewer sugar groups by exohydrolases requires the assistance of sphingolipid activator proteins (3). Sphingolipid activator proteins A–D and the GM2 activator protein (GM2AP) are the five known accessory proteins involved in ganglioside catabolism (2). Genetic mutations resulting in exohydrolase or accessory protein inactivity cause a number of deadly lysosomal storage diseases, including Tay-Sachs disease (1).

GM2AP is an 18-kDa accessory protein required as a cofactor for the effective hydrolysis of GM2 to GM3. Fürst and Sandhoff proposed that GM2AP binds to intralysosomal vesicles containing GM2 and extracts GM2 from the bilayer, forming a protein-lipid complex in solution for proper orientation of the terminal GalNAc sugar for cleavage by Hexosaminidase A (4). Crystal structures of GM2AP reveal a novel β-cup topology formed from eight β-strands with a hydrophobic pocket (5–7). It is known that in vitro, GM2AP can bind and extract GM2 from micelles and from vesicles, forming a 1:1 complex in solution (8). In addition to stimulating GM2 degradation, GM2AP has also been shown to bind and transfer nonspecific glycolipids, phospholipids (8–10), and a fluorescently labeled dansyl lipid between vesicles (11). Whether transferring phospholipid or ganglioside ligands, a model for this process must include the partitioning of GM2AP with the bilayer surface. Details of the molecular mechanism by which GM2AP extracts lipids from bilayers are still not well understood. It is postulated from the details of the crystal structures that an apolar loop spanning residues V59–W63 (highlighted in Fig. 1 *A*) inserts into the bilayer upon binding to the surface (5). However, monolayer studies indicate that GM2AP is only surface-associated to phosphatidylcholine bilayers and does not penetrate deeply into the bilayer (12). By determining the membrane-bound orientation of GM2AP, which includes identifying those residues that interact with the bilayer, we can gain insight into the mechanism of lipid extraction.

Site-directed spin-labeling electron paramagnetic resonance (EPR) spectroscopy has become a very powerful tool for studying both soluble and integral membrane proteins (13–26). In this method, site-specific amino acids of the protein are individually mutated to cysteine residues to which a nitroxide spin label is attached. Here, the methanethiosulfonate spin label (MTSL), which attaches to cysteines through a disulfide linkage and produces the modified side chain referred to as R1, has been used and the linkage scheme is shown in Fig. 1 *B*. Power saturation is an EPR-based technique that has been utilized for: determining the relative location of a spin label within lipid bilayers (13); studying accessibility of protein side chains to aqueous and lipid-soluble paramagnetic colliders (18,21,22); determining conformational changes of integral membrane proteins (23,24); and determining orientations of proteins on or within bilayers (15,25,26). Within this method,

Submitted March 30, 2009, and accepted for publication May 11, 2009.

*Correspondence: fanucci@chem.ufl.edu

Editor: David D. Thomas.

0006-3495/09/09/1436/9 $2.00

doi: 10.1016/j.bpj.2009.05.058

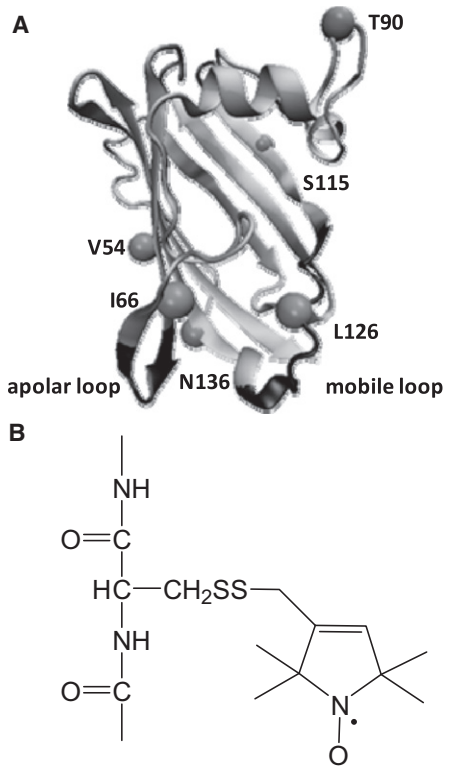

FIGURE 1 (*A*) Ribbon diagram of GM2AP (PDB ID 1G13) with sites mutated to cysteine residues for spin labeling with methanethiosulfonate shown by beads at the Cα position, the apolar (V59-W63) and mobile (P124-N136) putative membrane binding loops highlighted in dark gray. (*B*) Scheme for attaching the MTSL spin label to mutant cysteine residues via disulfide bond formation producing a modified side chain referred to as R1.

paramagnetic colliders of differing solubilities in the polar and nonpolar phases are utilized for discriminating the location of a spin label, where changes in the measured relaxation properties of the spin label correlate with collision frequency between the spin label and the paramagnetic collider (13). Examples of proteins whose orientations on bilayer surfaces have been characterized with the power saturation methodology include the C2 domains of cPLA2 and Synaptotagmin (14,15,17) and the human group IIA phospholipase A_2 (25).

Here, power saturation SDSL EPR spectroscopy is utilized to characterize, at low resolution, the orientation of GM2AP on 1-palmitoyl-2-oleoyl-*sn*-glycero-3-phosphocholine (POPC) bilayer surfaces. A series of six single cysteine variants of GM2AP were generated (Fig. 1 *A*), and each was expressed, purified, and spin labeled. Concurrent with our power saturation experiments, we have also characterized the binding interactions of GM2AP with POPC vesicles by sucrose-loaded vesicle sedimentation and fluorescence assays. Results show that GM2AP establishes bilayer partitioning where 15% of the protein remains on the bilayer surface with 85% in solution, mostly as a protein-lipid complex (27). Fig. 2 depicts this model where GM2AP establishes a series of equilibria, with the first being the

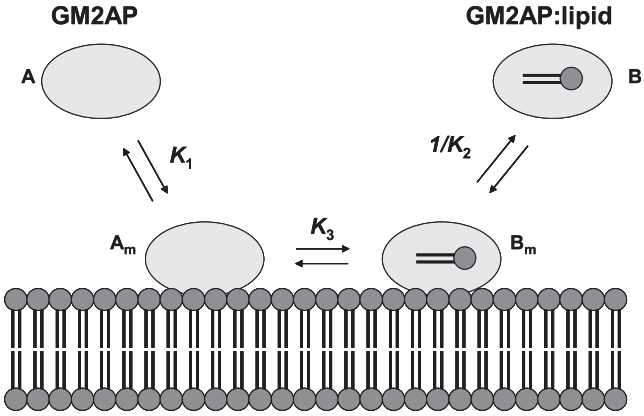

FIGURE 2 Cartoon showing a proposed mechanism for how GM2AP interacts with lipid vesicles, where equilibrium is established with apo protein in solution [A] or associated with the bilayer surface [A_m], or as a protein:lipid complex that is bound [B_m] to lipid bilayers or a protein:lipid complex in solution [B].

binding equilibrium with lipid vesicles (K_1) where the protein recognizes the lipid ligand (K_3), which then undergoes an equilibrium dissociation ($1/K_2$) from the vesicle surface as a protein-lipid complex. This finding was unexpected, because it was believed that GM2AP could only extract gangliosides from lipid vesicles when the unique endosomal lipid bis(monoacylglycerol)phosphate was present in the lipid composition (3). The results from the traditional power saturation experiments with water-soluble paramagnetic colliders, such as nickel ethylenediamine diacetic acid (NiEDDA), are consistent with our recent findings that GM2AP interacts transiently with the bilayer surface of POPC, establishing an equilibrium where only a small percentage of the protein remains on the bilayer surface.

Because of this partitioning, results from traditional power saturation with NiEDDA and oxygen did not provide useful constraints for determining the orientation of the membrane-bound state. Instead, a variation of the traditional power saturation method was employed, which utilizes the nickel-chelating lipid DOGS-NTA-Ni as a surface-bound paramagnetic collider. With this method, relaxation induced by only the surface-bound state is detected, so those sites that collided with the DOGS-NTA-Ni can be mapped onto the crystal structure, thereby providing a low-resolution model for how GM2AP orients on the POPC bilayers. These results show that GM2AP binds such that the entire face of the protein containing the lipid-binding pocket lies onto the bilayer surface. This orientation differs from that proposed from the x-ray structure but is consistent with other models of lipid binding proteins, including Sec14p (28,29).

MATERIALS AND METHODS

Materials

1-Palmitoyl-2-oleoyl-*sn*-glycero-3-phosphocholine (POPC) in chloroform, and 1,2-dioleoyl-*sn*-glycero-3-[(*n*-(5-amino-1-carboxypentyl)iminodiacetic

acid)succinyl] (Nickel salt, in chloroform) (DOGS-NTA-Ni) were purchased from Avanti Polar Lipids (Alabaster, AL) and used without further purification. *N*-(5-dimethylaminonaphthalene-1-sulfonyl)-1,2-dihexadecanoyl-*sn*-glycero-3-phosphoethanolamine, triethylammonium salt (DDHPE) was purchased from Molecular Probes (Eugene, OR) in the form of powder. Methanethiosulfonate spin label (MTSL) was purchased from Toronto Research Chemicals (North York, Ontario, Canada). Unless otherwise stated, all other reagents were from Fisher Scientific (Hampton, NH) and used as received.

Preparation of lipid vesicles

Lipid vesicles comprised of POPC, POPC:DOGS-NTA-Ni (9:1 molar ratio), and POPC:DDHPE (4:1 molar ratio) were prepared by mixing appropriate volumes of stock solution of POPC, DOGS-NTA-Ni, or DDHPE in chloroform, removing the organic solvent by drying under nitrogen stream and vacuum-desiccating overnight. Two separate samples of POPC LUVs were prepared. The first was rehydrated in 50 mM ammonium acetate (NH_4Ac) pH 4.5 buffer, and the second was rehydrated in 50 mM NH_4Ac pH 4.5 buffer containing 50 mM final concentration of NiEDDA. POPC:DOGS-NTA-Ni (9:1) lipid films were rehydrated by vortexing in 50 mM NH_4Ac pH 4.5 buffer; POPC:DDHPE (4:1) lipids were rehydrated by vortexing in 50 mM sodium acetate pH 4.8 buffer. For all samples, rehydration proceeded for 15 min at room temperature with gentle vortex mixing. Large unilamellar vesicles (LUVs) of the above lipid samples were prepared by extrusion consisting of 55 passes through 100-nm polycarbonate filters using an Avanti hand-held miniextruder (Alabaster, AL). Stock solutions of POPC and POPC:DOGS-NTA-Ni (9:1) LUVs were prepared at 200 mM. Final lipid concentrations for power saturation experiments were 20 mM total lipid. For those samples containing NiEDDA, the final concentration of NiEDDA was 20 mM.

Dansyl extraction functional assay

To characterize the function of the CYS-spin-labeled GM2AP constructs, an assay based upon DDHPE extraction was utilized (11). Here, function is defined as ability of GM2AP to bind to lipid vesicles and extract DDHPE to form a GM2AP:DDHPE complex in solution. The formation of the complex is followed with fluorescence spectroscopy. Further details are given in the Supporting Material.

Protein expression and purification of GM2AP mutants

Recombinant GM2AP WT and cysteine mutant constructs prepared using an *Escherichia coli* expression system as described in an earlier report (11) and was a modified procedure originally published by Wright et al. (5). Details of the spin-labeling procedure are given in the Supporting Material.

CW-EPR solution data collection

Continuous wave (CW) EPR spectra were collected on modified Bruker ER200 spectrometer (Billerica, MA) with an ER023M signal channel and an ER032M field control unit, and equipped with a loop gap resonator (Medical Advances, Milwaukee, WI). Solution spectra of GM2AP mutants were recorded with protein samples in sealed round capillaries, 0.60 mm × 0.84 mm × 100 mm (Fiber Optics Center, New Bedford, MA), at room temperature and with 3.16 mW incident power. Concentrations of protein ranged from 100 to 200 μM in either 50 mM Tris pH 8.0 or 50 mM NH_4Ac pH 4.5 buffers. LabVIEW software (National Instruments, Austin, TX) was used for baseline correction, and double integral area normalization, and was generously provided by Drs. Christian Altenbach and Wayne Hubbell (University of California at Los Angeles, Los Angeles, CA).

Power saturation EPR experiments

Two different sets of power saturation experiments are presented in this work:

1. The traditional power saturation experiment utilizing oxygen and NiEDDA colliders and
2. Power saturation using DOGS-NTA-Ni lipid as the paramagnetic collider.

Traditional power saturation experiments were collected at both pH 4.5, where GM2AP binds to lipid vesicles, and at pH 8.0, where GM2AP is unbound (27). Spin-labeled GM2AP mutants in 50 mM NH_4Ac pH 4.5 buffer or 50 mM Tris pH 8.0 buffer were mixed with POPC LUVs (50 mM NH_4Ac pH 4.5) or with POPC LUVs in 50 mM NH_4Ac pH 4.5 containing a final concentration of 20 mM NiEDDA. Final concentrations of protein and lipid were 120 μM and 20 mM, respectively. For pH 8.0 samples, the stock concentrations of protein (pH 8.0) and lipid (pH 4.5) were such that the sample after mixing protein with lipid was pH >7, which is sufficient for GM2AP to remain unbound. EPR spectra were collected from samples placed in gas-permeable TPX capillary tubes (Molecular Specialties Medical Advances, Milwaukee, WI) and equilibrated with either nitrogen gas or air (20% oxygen). The peak-to-peak first derivative amplitude, A_{pp}, of the central resonance ($m_I = 0$) was measured and plotted as a function of microwave power, P, ranging from incident power of 0.2–63 mW. The resultant curves were fit to the expression

$$A_{pp}(0) = I\sqrt{P}\left[1 + (2^{-\varepsilon} - 1)\frac{P}{P_{1/2}}\right]^{-\varepsilon}, \qquad (1)$$

where I is a scaling factor, $P_{1/2}$ is the power at which the resonance amplitude is one-half its unsaturated value, and ε is a measure of the homogeneity of the saturation of the resonance (13). $P_{1/2}$ values were obtained under three different sample conditions for samples at both pH 4.5 and pH 8.0 (a total of six power saturation experiments):

1. Protein mixed with POPC LUVs equilibrated in nitrogen gas.
2. Protein mixed with POPC LUVs equilibrated in lipid soluble air (20% oxygen).
3. Protein mixed with POPC LUVs with aqueous soluble 20 mM NiEDDA equilibrated in nitrogen.

$\Delta P_{1/2}$ values were obtained by subtracting the $P_{1/2}$ value for nitrogen from the $P_{1/2}$ values of oxygen and NiEDDA. Collision parameters, Π, for oxygen and NiEDDA were calculated according to

$$\Pi^{Oxy} \equiv \frac{\Delta P'_{1/2}(Oxy)}{P'_{1/2}(DPPH)} = \frac{P_{1/2}(Oxy)/\Delta H_{pp}(Oxy) - P_{1/2}(N_2)/\Delta H_{pp}(N_2)}{P_{1/2}(DPPH_2)/\Delta H_{pp}(DPPH_2)}. \qquad (2)$$

The Π-values for NiEDDA were calculated by substituting $P_{1/2}$(NiEDDA) for $P_{1/2}$(Oxy) in Eq. 2. The Π-values for DOGS-NTA-Ni were calculated by substituting $\Delta P_{1/2}$(DOGS) for $P_{1/2}$(Oxy) in Eq. 2.

A separate set of power saturation experiments utilizing DOGS-NTA-Ni as the paramagnetic collider were also performed under the following three conditions: pH 4.5, pH 4.5 + ethylenediaminetetraacetic acid (EDTA), and pH 8.0 (all under a nitrogen atmosphere). Spin-labeled GM2AP mutants in 50 mM NH_4Ac pH 4.5 buffer or 50 mM Tris pH 8.0 buffer were mixed with POPC:DOGS-NTA-Ni (9:1) LUVs in 50 mM NH_4Ac pH 4.5 buffer to give final protein and lipid concentrations of 120 μM and 20 mM, respectively. Two additional samples were also prepared for measuring the relaxation properties of each spin-labeled site in absence of collider that contained GM2AP mutants in both pH 4.5 and pH 8 buffers with POPC LUVs in 50 mM NH_4Ac pH 4.5 buffer. Final protein and lipid concentrations were

as described above. $P_{1/2}$ values (Eq. 1) were measured for GM2AP mutants mixed with POPC:DOGS-NTA-Ni (9:1) LUVs and for GM2AP mutants with POPC LUVs. $\Delta P_{1/2}$ values were obtained by subtracting the $P_{1/2}$ value for GM2AP with POPC in nitrogen from the $P_{1/2}$ values of GM2AP mutants with POPC:DOGS-NTA-Ni (16), and is shown as

$$\Delta P_{1/2}(\text{DOGS}) = P_{1/2}(\text{DOGS-NTA-Ni}) - P_{1/2}(\text{POPC}). \quad (3)$$

Power saturation data for the pH 4.5 + EDTA experiments were collected on the same samples used at pH 4.5. Here, 2 μL of 0.5 M EDTA solution was added to the 10-μL samples containing POPC:DOGS-NTA-Ni (9:1), to remove the nickel from the NTA chelator group, which is covalently attached to DOGS-NTA-Ni lipid, and the power saturation experiment was repeated with equilibration in nitrogen gas. $\Delta P_{1/2}$ values were obtained by subtracting the $P_{1/2}$ value for GM2AP with POPC in nitrogen from the $P_{1/2}$ values of GM2AP mutants with POPC:DOGS-NTA-Ni + EDTA.

RESULTS

Six sites of GM2AP (V54C, I66C, T90C, S115C, L126C, N136C) were chosen for single amino-acid substitution to cysteine for subsequent spin labeling. These spin-labeled sites were used to determine what regions of GM2AP interact with the lipid bilayer surface. The locations of the cysteine mutation sites are shown as spheres in the ribbon diagram of GM2AP in Fig. 1 *A*. The function of GM2AP spin-labeled mutant constructs, defined as the ability to extract the fluorescently labeled lipid DDHPE from LUVs, was assayed as described in an earlier report (11). From these experiments, the $t_{1/2}$ values for DDHPE extraction for spin-labeled GM2AP constructs were compared to WT and are given in Table 1. Spin-labeled mutants extract DDHPE from POPC LUVs at a rate that was within error of WT with a few exceptions. V54R1 extracted DDHPE slightly faster than WT ($t_{1/2} = 1.5 \pm 0.1$ min), whereas S115R1 and I66R1 extracted DDHPE slower than WT (Supporting Material).

EPR spectral line shapes for the R1-labeled GM2AP are shown in Fig. 3. Two spin-labeled sites, L126R1 and N136R1, are both located in one of the two putative lipid-bilayer binding loops and have EPR line shapes characteristic of spin labels in aqueous exposed flexible regions on proteins (30). I66R1 is located on the other putative binding loop and has a line shape with a broad component reflecting possible tertiary contact of R1 with neighboring residues around the lipid-binding cleft. The broadened line shape for I66R1 suggests that R1 may sterically interfere with DDHPE extraction, thus the longer half-life value for DDHPE extraction. Sites V54R1 and S115R1 are located on the back side of β-strands β-4 and β-6, respectively, and their EPR line shapes are slightly broadened, consistent with the attachment of R1 to a rigid portion of the protein. The spectrum of T90R1 is the narrowest line shape observed

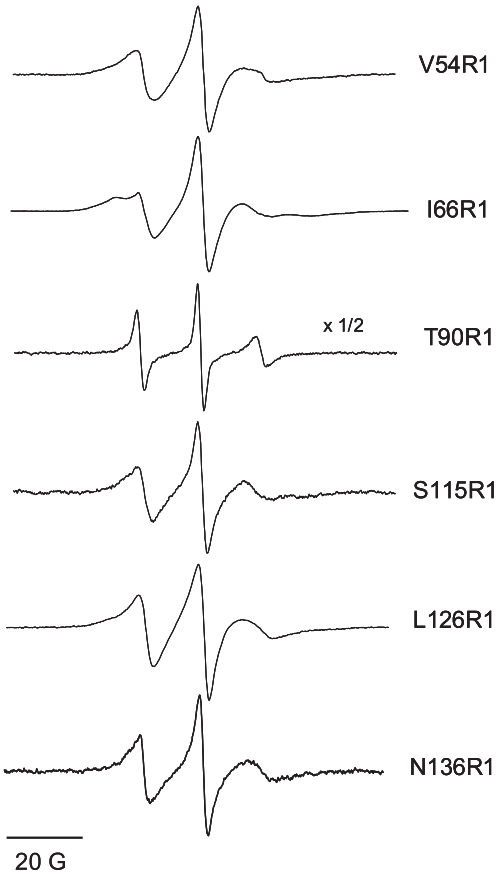

FIGURE 3 X-band continuous wave EPR spectra of the GM2AP R1 labeled CYS constructs in 50 mM Tris buffer, pH 8.0 at ambient temperature. Spectra are shown as 100 Gauss (G) scans and are plotted as double-integral area-normalized for easy comparison of spectral line shapes.

TABLE 1 Values of half-life for DDHPE extraction from POPC LUVs and collision parameters for GM2AP WT and R1 spin-labeled constructs

Mutant	$t_{1/2}$ (minutes)	Π^{oxy}_{lipid}	Π^{NiEDDA}_{lipid}	Π^{DOGS}	$\Pi^{DOGS + EDTA}$
WT	1.5 ± 0.1	—	—	—	—
V54R1	0.9 ± 0.1	0.14 ± 0.06	0.52 ± 0.07	0.09 ± 0.05	0.10 ± 0.04
I66R1	NA*	0.43 ± 0.07	1.14 ± 0.08	0.07 ± 0.05	0.09 ± 0.04
T90R1	1.8 ± 0.2	0.42 ± 0.07	1.04 ± 0.10	0.48 ± 0.05	0.10 ± 0.03
S115R1	5.2 ± 0.8	0.40 ± 0.12	0.57 ± 0.15	0.08 ± 0.11	0.06 ± 0.05
L126R1	1.7 ± 0.1	0.30 ± 0.04	0.30 ± 0.12	0.44 ± 0.06	0.01 ± 0.04
N136R1	1.6 ± 0.3	0.39 ± 0.07	0.97 ± 0.08	0.37 ± 0.10	0.20 ± 0.06

Note that dansyl extraction assays were performed at pH 4.8 with 5 μM final protein concentration and 1 μM final lipid concentration at 20°C.
*The DDHPE extraction could not be measured; no significant change in fluorescence signal was detected.

for those sites investigated here, indicating a high degree of mobility. This mobility is expected, given its location in a loop structure and high B-factors observed in the x-ray structure (5). Each of the spin-labeled sites has a line shape that is expected from comparison to the crystal structure. Interestingly, the EPR line shapes did not change within signal/noise when POPC vesicles were added. If the line shapes of GM2AP in solution are compared with line shapes in the membrane-binding loop regions of C2 domains (14,17), most of the solution spectra of GM2AP (excluding T90R1) more closely resemble the broadened line shapes of the C2 domain bound to the bilayer. Changes in EPR spectra were seen for C2 domains upon membrane binding because the loops are highly flexible in solution and become broadened upon penetration into the lipid bilayer. For GM2AP, the regions that contact the bilayer (described below) appear to be more motionally restricted compared to the loops of the C2 domains, and it is also likely that GM2AP does not penetrate deeply into the bilayer, consistent with Langmuir-monolayer studies that showed GM2AP remains surface-associated and does not penetrate deeply into the bilayer (12).

Power saturation EPR experiments were performed for each of the R1-labeled constructs with lipid vesicles in attempts to determine the membrane-bound orientation of GM2AP. Given that GM2AP functions at acidic pH, samples containing 20 mM POPC LUVs were prepared at pH 4.5. Values of oxygen accessibility (Π^{Oxy}) and NiEDDA accessibility (Π^{NiEDDA}) parameters were calculated from the power saturation curves and are reported in Table 1. By plotting Π^{NiEDDA} versus Π^{Oxy}, a correlation between collision parameters with spin-label location in either the aqueous or lipid phases can be obtained (15,31). Sites that are known to reside within the bilayer, such as DOXYL labels in phospholipids acyl chains and spin-labeled bacteriorhodopsin, cluster in one region of the graph, whereas the aqueous exposed sites of the C2 domain of cPLA2 result in values that cluster in another region. Fig. 4 shows this correlation and also plots the collision parameters obtained for GM2AP. The data points for GM2AP fall outside the boundaries. At first, this result was surprising, but it is consistent with our recent findings showing that GM2AP establishes an effective bilayer partitioning where ~15% GM2AP remains bound to the bilayer surface, regardless of lipid concentration (11,27). The inability to generate a sample where >99% of the protein is on the bilayer surface has a significant impact on the interpretation of the power saturation data.

The equilibrium exchange can explain why the data correlating the collision parameters Π^{Oxy} and Π^{NiEDDA} for GM2AP fall outside of the defined regions of the graph. In the oxygen experiment, changes in saturation are detected for those protein molecules bound to the POPC bilayer. The values obtained for Π^{Oxy} indicate that certain sites are located near the bilayer interface. However, in the NiEDDA experiment, the Π^{NiEDDA} values are dominated by collisions with GM2AP in solution. Currently, we do not know the exchange rate of the protein on and off the bilayer, but we assume it is much slower than the nanosecond timescale of the paramagnetic relaxation. Due to the partitioning behavior of GM2AP, the results from the traditional power saturation experiments could not be utilized for determining an orientation on bilayer surfaces, as has been done for C2 domains. Nevertheless, these data uphold our recent findings describing the bilayer partitioning and lipid extraction behavior of GM2AP.

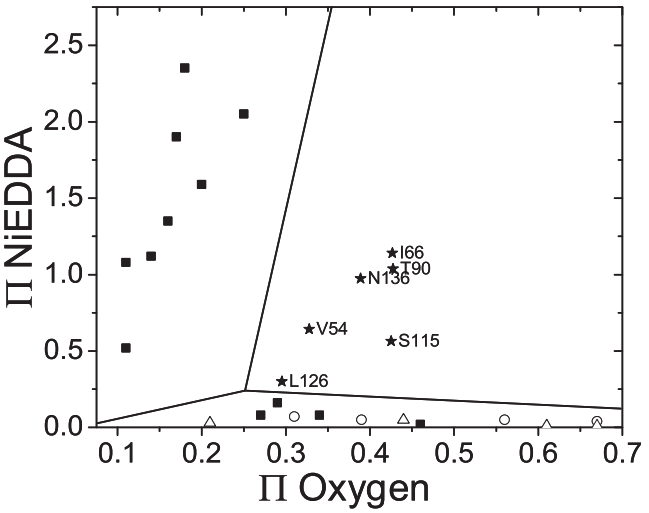

FIGURE 4 Plot of collision parameters, Π, for spin-labeled sites of GM2AP (*solid stars*), of C2 domain of cPLA2 bound to PC/PS bilayers (3:1) (*solid squares*), of bacteriorhodopsin (*open triangles*) and of doxyl-labeled lipids (*open circles*). Plotting Π^{NiEDDA} versus Π^{Oxygen} has been used to differentiate aqueous exposed sites from sites buried within the lipid bilayer based on where the points cluster on the graph. The aqueous exposed sites occupy the upper-left region of the plot and the lipid exposed sites fall in the lower region along the *x* axis. All spin-labeled sites of GM2AP gave collision data that placed them outside the defined regions of the Π^{NiEDDA} versus Π^{Oxygen} plot. Data points for the C2 domain and bacteriorhodopsin were taken from Frazier et al. (15) and Hubbell et al. (31), respectively.

Mapping the membrane-bound orientation of GM2AP with DOGS-NTA-Ni

Because GM2AP partitions on and off the surface and can extract POPC, a surface-bound collider was utilized to map those sites in GM2AP that come into contact with the POPC vesicle surface during binding/lipid extraction. The lipid DOGS-NTA-Ni has a linker that extends from the phosphate headgroup into solution a maximum distance of 14 Å (16). This lipid has been previously utilized to characterize surface-located residues in the integral membrane protein KcsA (16) and to investigate the interactions of the cytoplasmic domain of phospholamban with sarcoplasmic reticulum Ca^{2+}-ATPase (22). Here, DOGS-NTA-Ni was incorporated into POPC bilayers to serve as a surface-bound paramagnetic collider in the power saturation experiments such that relaxation would occur for only those sites that were interacting with the bilayer surface. Control experiments

(shown in the Supporting Material) demonstrate that although GM2AP can extract POPC and other phospholipids, GM2AP cannot extract DOGS-NTA-Ni from the vesicles. $\Pi^{DOGS\text{-}NTA\text{-}Ni}$ values were determined as described in Eq. 3. Fig. 5 shows power saturation curves obtained for the spin-labeled GM2AP mutants mixed with DOGS-NTA-Ni containing LUVs purged with a nitrogen background for pH 8, pH 4.5, and pH 4.5 with EDTA. Very low values ($\Pi < 0.1$) were seen for all spin-labeled positions at pH 8 as expected, because at this pH, GM2AP remains unbound (27). At pH 4.5, surface collisions of GM2AP showed accessibility to DOGS-NTA-Ni for sites T90R1, L126R1, and N136R1, as seen by larger collision values ($\Pi > 0.1$) compared to those obtained at pH 8. Because the larger $\Pi^{DOGS\text{-}NTA\text{-}Ni}$ values result from higher frequencies of collision of the spin label with the surface-bound collider, it is evident that these three sites interact with the bilayer surface. Sites V54R1, I66R1, and S115R1 had low $\Pi^{DOGS\text{-}NTA\text{-}Ni}$ values ($\Pi < 0.1$) at acidic pH. Although these low values can indicate that these GM2AP constructs did not bind to the LUVs, the DDHPE extraction assay for V54R1 and S115R1 confirm function; therefore, the power saturation results are interpreted to mean that

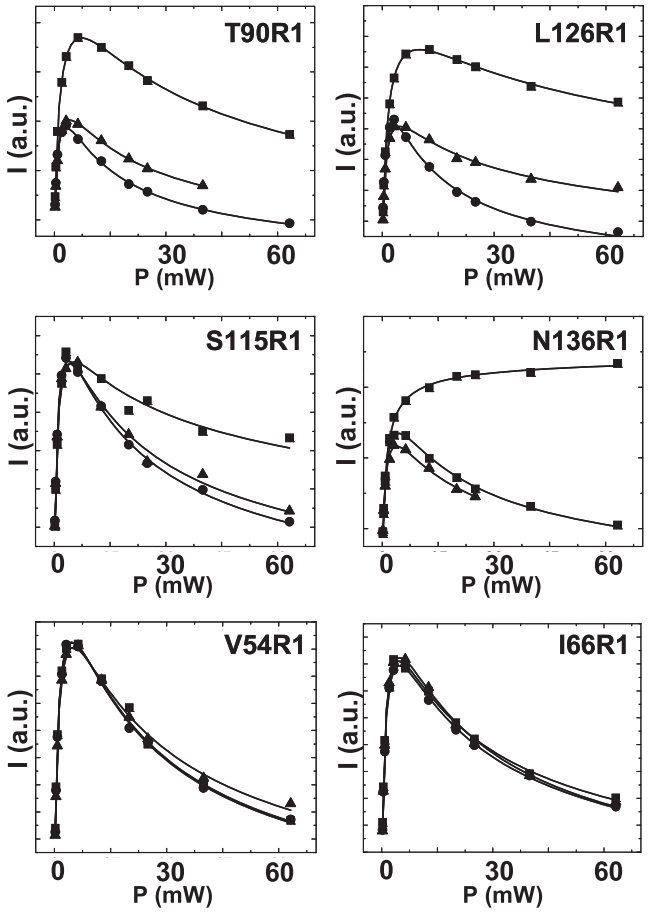

FIGURE 5 Power saturation curves for GM2AP R1 constructs mixed with POPC/DOGS-Ni-NTA(9:1) LUVs under three different experimental conditions: pH 8 (▲), pH 4.5 (■), and pH 4.5 + EDTA (●).

GM2AP binds to vesicles in an orientation that makes R1 at these three sites inaccessible to collision with DOGS-NTA-Ni.

Our proposed membrane-bound orientation positions I66R1 near the bilayer surface (discussed below), but R1 at I66C showed very low collision values with DOGS-NTA-Ni. This finding, along with the relatively broadened I66R1 spectral line shape and the high collisions with oxygen when power saturation was performed on protein in solution (data not shown), are consistent with a model where the spin label is tucked in toward the hydrophobic cavity. It is also likely that the A60 apolar loop that contains I66, seen in an extended conformation in the crystal structure, is due to crystal-crystal contacts in the unit cell. High collisions to oxygen in solution can arise from local high concentrations of oxygen within the hydrophobic interior pocket of GM2AP. In addition, spin-labeled I66C extracts DDHPE from vesicles slower than WT, a finding also consistent with the spin label tucked into the hydrophobic binding pocket, sterically blocking the opening to the cavity likely, preventing DDHPE from entering. Interestingly, although the spin label at site I66C prevents the extraction of DDHPE, we find that the I66R1 construct can extract the functional ganglioside ligand, GM2, from POPC:GM2 (3:1) LUVs (Supporting Material). Sites T90C and L126C showed the largest $\Pi^{DOGS\text{-}NTA\text{-}Ni}$ values indicating the closest contact with the bilayer. Site T90C is particularly significant because the strong collisions of R1 with DOGS-NTA-Ni at this site suggest an orientation of lipid binding that is different from the proposed conformation based upon analysis of hydrophobic regions of the protein in the x-ray structures (5,32,33). For all sites, after performing the power saturation experiment at pH 4.5, an excess of EDTA was added to the sample to remove the nickel from the surface, and the power saturation was repeated. Removal of surface-bound collider resulted in decreased relaxation enhancement of the spin label and, therefore, resulted in lower $\Pi^{DOGS\text{-}NTA\text{-}Ni+EDTA}$ values than those obtained at pH 4.5 without EDTA. For all spin-labeled sites, the power saturation curves for DOGS-NTA-Ni with EDTA resembled those for unbound GM2AP (pH 8). This decrease in $\Pi^{DOGS\text{-}NTA\text{-}Ni+EDTA}$ values upon addition of EDTA confirms the protein's association with lipid bilayers.

We can compare $\Pi^{DOGS\text{-}NTA\text{-}Ni}$ values obtained in this study to values published for KcsA (16). Fig. 6 is a plot of $(\Pi^{DOGS\text{-}NTA\text{-}Ni})^{-1}$ versus $(\Pi^{Oxy})^{-1}$ for GM2AP (*solid diamonds*) and for KcsA (*open circles*). For both GM2AP and KcsA, sites of high collisions with DOGS-NTA-Ni have similar Π-values and occur at the lipid-aqueous interface where the spin labels are the most accessible to the surface-bound collider. Decreased values of collision parameters are observed for spin-labeled sites in KcsA that move further into the bilayer. For GM2AP, the sites with low Π-values arise from an orientation of the protein on the bilayer surface that positions the spin labels so that they are unable to physically collide with DOGS-NTA-Ni, or, for

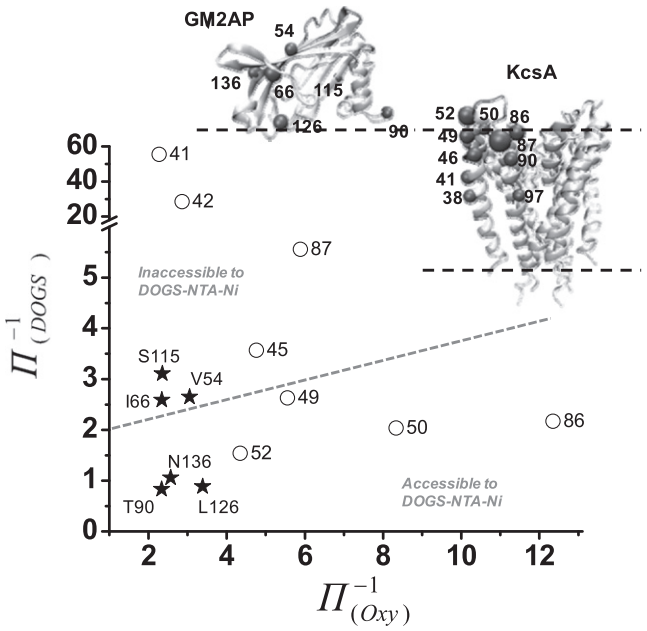

FIGURE 6 Inverse plot of $\Pi^{\text{DOGS-NTA-Ni}}$ versus Π^{Oxy} for spin-labeled GM2AP sites shown as solid diamonds and KcsA sites shown as open circles. Crystal structures of both GM2AP (PDB ID 1G13) and KcsA (PDB ID 1BL8) with the Cα positions of sites of spin-label attachment are shown as spheres. Collision values for KcsA with DOGS-NTA-Ni were taken from Gross and Hubbell (16), and oxygen collision values were taken from Perozo et al. (24). The line provides a general separation of data points that were found to be accessible and inaccessible to DOGS-NTA-Ni as defined for KcsA. Spin-labeled sites of KcsA that were inaccessible to DOGS-NTA-Ni were located on the transmembrane helices that were within the bilayer, and therefore, had larger oxygen collision values. GM2AP is surface-associated to lipid bilayers, and spin-labeled sites of GM2AP that were inaccessible to DOGS-NTA-Ni were not in the bilayer, as seen for KcsA. The inaccessible sites of GM2AP were located in the aqueous phase rather than the bilayer, which resulted in lower oxygen collisions compared to KcsA.

the case of I66R1, where the label is tucked into the hydrophobic pocket or protected at the bilayer interface. From mapping the relative accessibility to DOGS-NTA-Ni for various sites of GM2AP, we propose a model where GM2AP sits on the bilayer with the face of the hydrophobic pocket pointing toward the phospholipid surface. This orientation differs from the original hypothesized model that suggested that the protein bound to bilayers in an upright fashion so that the apolar loop inserted into the bilayer (5,32,33). The high collision value for T90R1 with DOGS-NTA-Ni means that this site is close to the bilayer surface, and that constraint was not accommodated by the hypothesized model. Additionally in the x-ray model, V54 and S115 would be expected to have moderate collisions with DOGS-NTA-Ni, which is not observed. Fig. 7, *A* and *B*, shows the x-ray and EPR orientations of GM2AP on lipid bilayers to distinguish the original model from the one determined from these power saturation studies. Again, spheres represent sites mutated to CYS for EPR measurements and the color code indicates the relaxation values of $\Pi^{\text{DOGS-NTA-Ni}}$. It is clear from Fig. 7, *A* and *B*, that T90R1 in the original model would be inaccessible to DOGS-NTA-Ni, as it is positioned far from the bilayer surface.

DISCUSSION

In addition to functioning as an accessory protein in ganglioside breakdown, GM2AP, in vitro, can transfer phospholipids (34) and fluorescent lipids (11) between vesicles, and can bind and consequently inhibit platelet activating factor (6), as well as participate in presenting lipid antigens to T-cells (35). Each of these functions involves binding and extracting lipids from bilayers, but the mechanistic details of lipid extraction are not known.

Power saturation EPR spectroscopy has been used as a structural biology tool for determining surface-bound orientations of numerous membrane binding proteins including human group IIA phospholipase A_2 (25) and C2 domains (14,17). This methodology has advanced from measuring the depth of spin-labeled proteins in bilayers to providing intricate details of Euler angle rotations of the

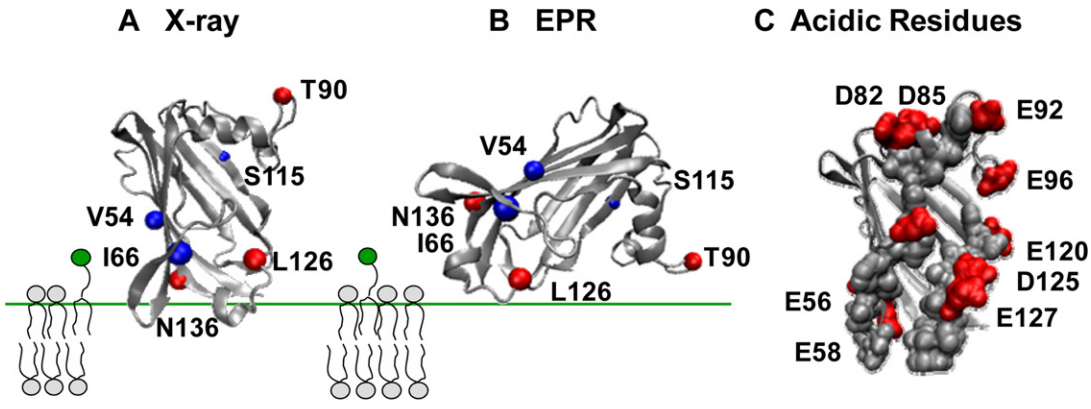

FIGURE 7 (*A*) Model of the membrane-bound orientation of GM2AP proposed from x-ray structure analysis (5,32,33) and, (*B*) the orientation of GM2AP on POPC bilayers after power saturation experiments, showing sites of high collisions (*red*) and low collisions (*blue*) to DOGS-NTA-Ni. The DOGS-NTA-Ni lipid is represented by the cartoon lipid containing the green sphere. (*C*) Ribbon diagram of GM2AP with the acidic residues shown in red and nonpolar residues in gray. The acidic residues that surround the hydrophobic cup may act as a pH switch for GM2AP binding to bilayers.

membrane docked protein. Here, we do not report a high-resolution orientation of GM2AP on POPC bilayers, but our collisional data with DOGS-NTA-Ni does provide evidence that the protein is rotated such that the face of the hydrophobic pocket interacts with the bilayer. This orientation differs from the model proposed from analysis of the x-ray structures (5,32,33), which postulated that the apolar loop (Fig. 1 *A* and Fig. 7) might penetrate into the bilayer.

Fig. 7, *A* and *B*, compares the orientation of GM2AP binding to lipid bilayers obtained from analysis of x-ray structures with the model that is more consistent with our EPR results. Sites of high and low collision with DOGS-NTA-Ni are highlighted in red and blue, respectively. Rotating the protein such that the high collision sites are nearest the bilayer and low collision sites are not in proximity for collisions with DOGS-NTA-Ni positions the residues lining the entire hydrophobic pocket on the bilayer surface. Although site N136 appears misplaced from the bilayer surface, we believe the x-ray conformation to be extended via crystal-crystal contacts, and that this loop is actually more tucked in the solution conformation. This orientation is plausible because it is known that lipids occupy the hydrophobic cavity, so its opening should face the bilayer in order for the lipids to enter the binding pocket. One side of the cavity entrance consists of a highly flexible region called the mobile loop and spans residues V122 to N136. This region of the protein was seen in various conformations in x-ray structures, where one conformation, presumably the open conformation, widens the opening to the cavity whereas in another conformation, the loop is tucked into the pocket and closes the entrance. We could propose from the surface-bound orientation and the dynamic nature of this stretch of amino acids that positioning the entire face of hydrophobic pocket creates a favorable environment for the phospholipid acyl tails to flip from the bilayer into the hydrophobic pocket of membrane-bound GM2AP, and that the opening and closing of the mobile loop could aid in facilitating lipid extraction.

We can compare our model of GM2AP lipid binding to information known about other lipid transfer proteins. Sec14p is a phosphatidylinositol transfer protein and has a hydrophobic phospholipid binding pocket that is thought to be gated by an α-helix. EPR studies by Smirnova et al. provided many important details to phospholipid binding (28). First, the orientation of the spin-labeled phospholipid positions the acyl tails within the cavity and the lipid headgroup points out toward solution. The flexibility of the acyl tails increased as distance from the headgroup increased down the *sn*-2 acyl chain, suggesting tighter binding at the headgroup region. These studies also revealed that Sec14p creates a polarity gradient that accommodates binding phospholipids, such that the interior of the protein, the part occupied by the ends of the acyl tails, is aprotic and gradually changes to a more protic environment around the lipid headgroup. This gradient was postulated to be the driving force of lipid extraction. Like Sec14p, GM2AP binds GM2 such that the acyl tails of the ceramide moiety of GM2 occupy the hydrophobic pocket and the oligosaccharide headgroup is solvent-accessible. Both of these proteins also share the feature of having a relatively spacious lipid binding pocket, as was demonstrated by mobility parameters of DOXYL-labeled lipids bound to Sec14p (28) and by measuring the dimensions of the hydrophobic cavity of GM2AP determined by analysis of the x-ray structure (5) although GM2AP has a larger binding pocket than Sec14p.

The orientation of GM2AP on the bilayer surface shown in Fig. 7 *B* is further supported by inspecting the specific residues that surround the cavity. A number of hydrophobic amino acids (valine, phenylalanine, and leucine), small polar amino acids (serine and threonine) as well as aspartic acid and glutamic acid residues line the binding pocket. Fig. 7 *C* highlights the acidic residues in red. The presence of hydrophobic residues is expected given that the protein interacts with lipid bilayers. It is interesting, however, that a number of aspartic acid and glutamic acid residues are also found in this region of GM2AP. At pH <5, it is likely that the majority of these acidic amino-acid side chains are protonated, which could then lower the Born repulsion energy needed for interaction with the lower dielectric medium of the bilayer. Protonated aspartates and glutamates are still polar, so deep penetration into the bilayer is not expected, but rather these side chains would be expected to associate with the phosphate-glycerol headgroup region of the lipid bilayer. If we consider that the collision data with DOGS-NTA-Ni show that GM2AP binds to bilayers at pH 4.5 and not at pH 8, it is apparent that these acidic residues act as a pH switch that modulates GM2AP binding to bilayers simply as a result of the charge state of the acidic amino-acid side chains. We believe these residues play a crucial role in driving binding to lipid bilayers at acidic pH.

Traditional power saturation experiments that use oxygen and NiEDDA colliders provide a means for measuring protein orientations on and within lipid bilayers and is a technique typically applied to studies of either integral membrane proteins or membrane proteins that remain bound to bilayers. This is the first report of using power saturation to study a protein that undergoes exchange on and off the bilayer surface. Incorporating a surface-bound paramagnetic collider through use of DOGS-NTA-Ni has allowed us to effectively take a snapshot of the orientation of the protein when bound to the bilayer. This strategy allows for the mapping of these regions of the protein that were accessible to collisions with DOGS-NTA-Ni, and leads to a low-resolution orientation of GM2AP on POPC bilayers, which was not attainable by the traditional method.

SUPPORTING MATERIAL

Three figures and one table are available at http://www.biophysj.org/biophysj/supplemental/S0006-3495(09)01151-5.

We are grateful to Dr. Christine Schubert Wright for providing us with the necessary plasmids for this work.

The research herein was funded by the National Institutes of Health No. R01GM077232 (G.E.F.)

REFERENCES

1. Gravel, R., J. Clarke, M. Kaback, D. Mahuran, K. Sandhoff, et al. 1995. The GM2 Gangliosidoses C. R. Scriver, A. L. Beaudet, W. S. Sly, and D. Valle, editors. McGraw-Hill, New York.
2. Sandhoff, K., and T. Kolter. 1996. Topology of glycosphingolipid degradation. *Trends Cell Biol.* 6:98–103.
3. Kolter, T., and K. Sandhoff. 2005. Principles of lysosomal membrane digestion: stimulation of sphingolipid degradation by sphingolipid activator proteins and anionic lysosomal lipids. *Annu. Rev. Cell Dev. Biol.* 21:81–103.
4. Fürst, W., and K. Sandhoff. 1992. Activator proteins and topology of lysosomal sphingolipid catabolism. *Biochim. Biophys. Acta.* 1126:1–16.
5. Wright, C. S., S. C. Li, and F. Rastinejad. 2000. Crystal structure of human GM2-activator protein with a novel β-cup topology. *J. Mol. Biol.* 304:411–422.
6. Wright, C. S., L. Z. Mi, and F. Rastinejad. 2004. Evidence for lipid packaging in the crystal structure of the GM2-activator complex with platelet activating factor. *J. Mol. Biol.* 342:585–592.
7. Wright, C. S., L. Z. Mi, S. Lee, and F. Rastinejad. 2005. Crystal structure analysis of phosphatidylcholine-GM2-activator product complexes: evidence for hydrolase activity. *Biochemistry.* 44:13510–13521.
8. Conzelmann, E., J. Burg, G. Stephan, and K. Sandhoff. 1982. Complexing of glycolipids and their transfer between membranes by the activator protein for degradation of lysosomal ganglioside GM2. *Eur. J. Biochem.* 123:455–464.
9. Mahuran, D. J. 1998. The GM2 activator protein, its roles as a co-factor in GM2 hydrolysis and as a general glycolipid transport protein. *Biochim. Biophys. Acta.* 1393:1–18.
10. Rigat, B., W. Wang, A. Leung, and D. J. Mahuran. 1997. Two mechanisms for the recapture of extracellular GM2 activator protein: evidence for a major secretory form of the protein. *Biochemistry.* 36:8325–8331.
11. Ran, Y., and G. E. Fanucci. 2008. A dansyl fluorescence-based assay for monitoring kinetics of lipid extraction and transfer. *Anal. Biochem.* 382:132–134.
12. Giehl, A., T. Lemm, O. Bartelsen, K. Sandhoff, and A. Blume. 1999. Interaction of the GM2-activator protein with phospholipid-ganglioside bilayer membranes and with monolayers at the air-water interface. *Eur. J. Biochem.* 261:650–658.
13. Altenbach, C., D. A. Greenhalgh, H. G. Khorana, and W. L. Hubbell. 1994. A collision gradient method to determine the immersion depth of nitroxides in lipid bilayers: application to spin-labeled mutants of bacteriorhodopsin. *Proc. Natl. Acad. Sci. USA.* 91:1667–1671.
14. Frazier, A. A., C. R. Roller, J. J. Havelka, A. Hinderliter, and D. S. Cafiso. 2003. Membrane-bound orientation and position of the Synaptotagmin I C2A domain by site-directed spin labeling. *Biochemistry.* 42:96–105.
15. Frazier, A. A., M. A. Wisner, N. J. Malmberg, K. G. Victor, G. E. Fanucci, et al. 2002. Membrane orientation and position of the C2 domain from cPLA2 by site-directed spin labeling. *Biochemistry.* 41:6282–6292.
16. Gross, A., and W. L. Hubbell. 2002. Identification of protein side chains near the membrane-aqueous interface: a site-directed spin labeling study of KcsA. *Biochemistry.* 41:1123–1128.
17. Herrick, D. Z., S. Sterbling, K. A. Rasch, A. Hinderliter, and D. S. Cafiso. 2006. Position of Synaptotagmin I at the membrane interface: cooperative interactions of tandem C2 domains. *Biochemistry.* 45:9668–9674.
18. Koteiche, H. A., M. D. Reeves, and H. S. McHaourab. 2003. Structure of the substrate binding pocket of the multidrug transporter EmrE: site-directed spin labeling of transmembrane segment 1. *Biochemistry.* 42:6099–6105.
19. Perozo, E., D. M. Cortes, P. Sompornpisut, A. Kloda, and B. Martinac. 2002. Open channel structure of MscL and the gating mechanism of mechanosensitive channels. *Nature.* 418:942–948.
20. Fanucci, G. E., and D. S. Cafiso. 2006. Recent advances and applications of site-directed spin labeling. *Curr. Opin. Struct. Biol.* 16:644–653.
21. Fanucci, G. E., N. Cadieux, C. A. Piedmont, R. J. Kadner, and D. S. Cafiso. 2002. Structure and dynamics of the β-barrel of the membrane transporter BtuB by site-directed spin labeling. *Biochemistry.* 41:11543–11551.
22. Kirby, T. L., C. B. Karim, and D. D. Thomas. 2004. Electron paramagnetic resonance reveals a large-scale conformational change in the cytoplasmic domain of phospholamban upon binding to the sarcoplasmic reticulum Ca-ATPase. *Biochemistry.* 43:5842–5852.
23. Dong, J., G. Yang, and H. S. McHaourab. 2005. Structural basis of energy transduction in the transport cycle of MsbA. *Science.* 308:1023–1028.
24. Perozo, E., D. M. Cortes, and L. G. Cuello. 1998. Three-dimensional architecture and gating mechanism of a K+ channel studied by EPR spectroscopy. *Nat. Struct. Biol.* 5:459–469.
25. Canaan, S., R. Nielsen, F. Ghomashchi, B. H. Robinson, and M. H. Gelb. 2002. Unusual mode of binding of human group IIA secreted phospholipase A_2 to anionic interfaces as studied by continuous wave and time domain electron paramagnetic resonance spectroscopy. *J. Biol. Chem.* 277:30984–30990.
26. Macosko, J. C., C. H. Kim, and Y. K. Shin. 1997. The membrane topology of the fusion peptide region of influenza hemagglutinin determined by spin-labeling EPR. *J. Mol. Biol.* 267:1139–1148.
27. Ran, Y., and G.E. Fanucci. Ligand extraction properties of the GM2 activator protein and its interactions with lipid vesicles. *Biophys. J.* 97:257–266.
28. Smirnova, T. I., T. G. Chadwick, R. MacArthur, O. Poluektov, L. Song, et al. 2006. The chemistry of phospholipid binding by the *Saccharomyces cerevisiae* phosphatidylinositol transfer protein Sec14p as determined by EPR spectroscopy. *J. Biol. Chem.* 281:34897–34908.
29. Smirnova, T. I., T. G. Chadwick, M. A. Voinov, O. Poluektov, J. van Tol, et al. 2007. Local polarity and hydrogen bonding inside the Sec14p phospholipid-binding cavity: high-field multi-frequency electron paramagnetic resonance studies. *Biophys. J.* 92:3686–3695.
30. McHaourab, H. S., M. A. Lietzow, K. Hideg, and W. L. Hubbell. 1996. Motion of spin-labeled side chains in T4 lysozyme. Correlation with protein structure and dynamics. *Biochemistry.* 35:7692–7704.
31. Hubbell, W. L., and C. Altenbach. 1994. Investigation of structure and dynamics in membrane proteins using site directed spin labeling. *Curr. Opin. Struct. Biol.* 4:566–573.
32. Wendeler, M., J. Hoernschemeyer, D. Hoffmann, T. Kolter, G. Schwarzmann, et al. 2004. Photoaffinity labeling of the human GM2-activator protein. Mechanistic insight into ganglioside GM2 degradation. *Eur. J. Biochem.* 271:614–627.
33. Wright, C. S., Q. Zhao, and F. Rastinejad. 2003. Structural analysis of lipid complexes of GM2-activator protein. *J. Mol. Biol.* 331:951–964.
34. Kuwana, T., B. M. Mullock, and J. P. Luzio. 1995. Identification of a lysosomal protein causing lipid transfer, using a fluorescence assay designed to monitor membrane fusion between rat liver endosomes and lysosomes. *Biochem. J.* 308:937–946.
35. Zhou, D., C. Cantu, 3rd, Y. Sagiv, N. Schrantz, A. B. Kulkarni, et al. 2004. Editing of CD1d-bound lipid antigens by endosomal lipid transfer proteins. *Science.* 303:523–527.